Single-Atom *O*-Bridged Urea in a Dinickel(II) Complex together with Ni_4^{II}, Cu_2^{II} and Cu_4^{II} Complexes of a Pentadentate Phenol-Containing Schiff Base with (O,N,O,N,O)-Donor Atoms

Soumen Mukherjee,[a] Thomas Weyhermüller,[a] Eberhard Bothe,[a] Karl Wieghardt,[a] and Phalguni Chaudhuri*[a]

Keywords: N,O ligands / Nickel / Copper / Magnetic properties / Radicals / Electrochemistry

A pentadentate phenol-containing ligand (H_3L) with N_2O_3 donor atoms yields Ni_2^{II} (**1**), Ni_4^{II} (**2**), Cu_2^{II} (**3**) and Cu_4^{II} (**4**) complexes, which have been structurally characterized by X-ray diffraction. Complex **1** contains a single-atom *O*-bridged urea. The compounds were characterized by IR, UV/Vis, mass spectrometry, electrochemistry and variable-temperature (2–295 K) magnetic susceptibility measurements. Analysis of the susceptibility data shows antiferromagnetic interactions between the metal centers indicating a diamagnetic ground state for complexes **1**, **3** and **4**, whereas complex **2**, a tetranuclear Ni^{II} cubane, has a complicated low-lying magnetic structure with a non-diamagnetic ground state. A plot of *J* vs. Ni–O–Ni angles for all structurally characterized Ni_4O_4 cubane cores, including **2**, irrespective of their symmetry exhibits a large variation of *J* values within a small range of Ni–O–Ni angles. The electrochemistry of all complexes was investigated in detail and the ligand-centered oxidation to a radical-ligand is inferred from the occurrence of oxidation processes at potentials which are similar.

Introduction

Polynuclear metal complexes are of current interest to chemists owing to their relevance to metallobiochemistry,[1] materials science[2] and theoretical chemistry.[3] Particular interest has been directed towards the exchange phenomena in di- and polynuclear complexes of nickel(II) and copper(II), in which studies, particularly of the latter, have led to essential insights into magnetostructural correlations.

Since the first report by Robson[4] in 1970 of a dinucleating Schiff-base ligand obtained by condensation of 2,6-diformyl-4-methylphenol with 2-aminophenol, many examples of similar compartmental ligands have been reported.[5] The dinucleating ability of these ligands stems from the readiness of the phenol to deprotonate and bridge two metal ions. Recently, we have reported trinuclear and tetranuclear complexes with the ligands derived from the condensation of 2,6-diformyl-4-methylphenol and selected diamines or hydroxylamines, which yield heteronuclear complexes of the type $M_AM_BM_C$ [6] and $M_AM_BM_BM_A$.[7]

In another field of coordination chemistry, interest in phenol-containing ligands was sparked and fueled by the discovery that tyrosyl radicals, derived from oxidation of the amino acid tyrosine, play an important role in a rapidly growing number of oxygen-dependent enzymatic radical catalysis reactions.[8] Since then chemists have attempted to model tyrosine by phenolate ligands.[9,10]

It has already been reported[10] that *tert*-butyl substituents at the *ortho* and *para* positions of the phenolates facilitate one-electron oxidation to the corresponding phenoxyl radicals, because these substituents decrease the oxidation potential of the phenolates and provide enough steric bulk to suppress bimolecular decay reactions of the generated phenoxyl radicals. Accordingly, we report here the synthesis and characterization of dinuclear and tetranuclear complexes of Ni^{II} and Cu^{II} ions with the Schiff-base ligand H_3LtBu derived from the (1+2) condensation of 2,6-diformyl-4-methylphenol and 6-amino-2,4-di-*tert*-butylphenol. A few square-planar dinickel(II) and dicopper(II) complexes have already been described by Robson,[4] but no structural data are available for these complexes, except one with the composition $[LCo^{II}Co^{III}(OH)(CH_3COO)]_2$.[11]

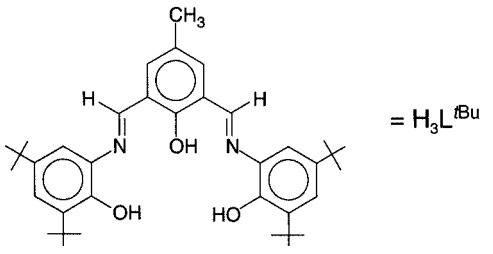

Scheme 1 shows the complexes of the ligand H_3LtBu prepared, along with their labels. Compounds **5**–**8** will not be described in this paper but in a subsequent one, and are

[a] Max-Planck-Institut für Strahlenchemie, Stiftstrasse 34–36, 45470 Mülheim an der Ruhr, Germany
E-mail: Chaudh@mpi-muelheim.mpg.de

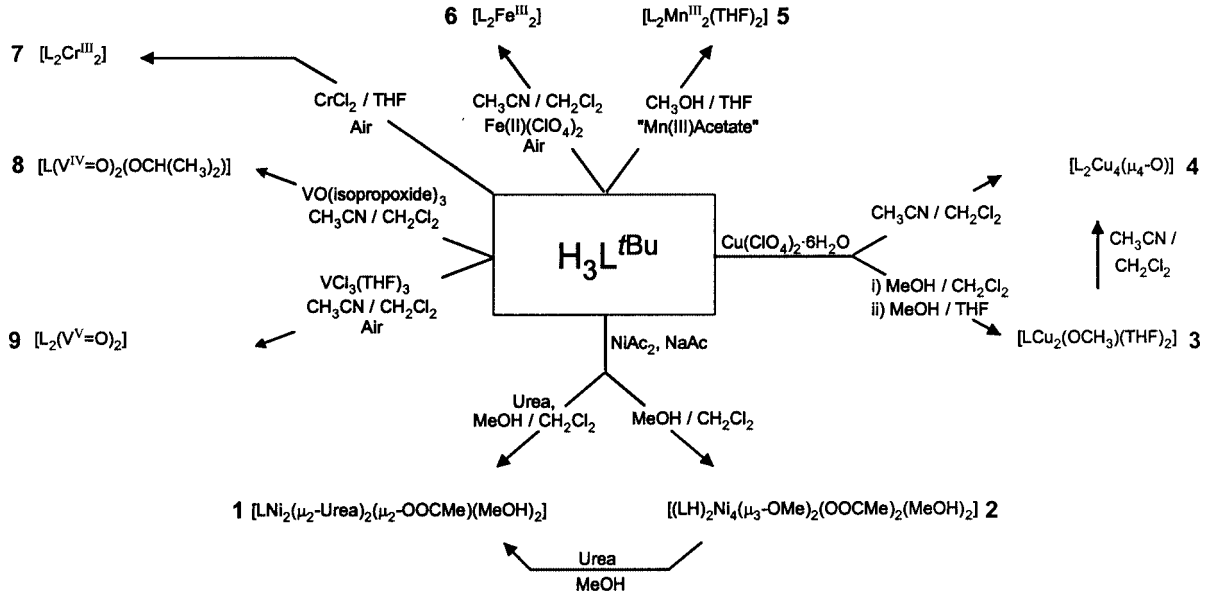

Scheme 1

mentioned here only to exemplify the diversified ligating properties of H_3LtBu. For the sake of simplicity the ligand will be denoted as H_3L without the suffix *t*Bu. We report here a dinuclear nickel(II) complex **1** with a bridging urea through a single-atom *O*-bridging of the carbonyl oxygen, as a model for a binding mode of the substrate urea in the nickel-dependent hydrolase enzyme urease (E.C. 3.5.1.5),[12−13] which is present in bacteria, fungi and higher plants, and catalyzes the hydrolysis of urea to ammonia and carbon dioxide.

$$H_2N\text{-}\underset{\underset{O}{\|}}{C}\text{-}NH_2 \xrightarrow[H_2O]{\text{urease}} 2\,NH_3 + CO_2$$

Several dinuclear nickel(II) complexes with urea[14] have been reported as models for possible binding modes of urea in urease. But none of the complexes reported so far, except one,[15] contain a carbonyl single-atom bridging urea.

Results and Discussion

When nickel acetate and H_3L are allowed to react in the presence of sodium acetate with a slight excess of urea in methanol, complex **1** is obtained. In the absence of urea, the tetranuclear complex **2** is obtained. Complex **2** can also be transformed into **1** by adding urea to the red solution of **2** in methanol (Scheme 1). Formation of **1** from **2** implies that the driving force for formation of **1** lies in the strong tendency of urea to bind to the dinickel center embedded in the dinucleating ligand L^{3-}. The solid-state FTIR spectrum of complex **1** exhibits a shift in the carbonyl stretching frequency of urea from 1690 to 1670 cm^{-1} upon coordination to the dinickel center. Mass spectrometry in the EI mode indicates unambiguously the presence of urea and an acetate ion in **1**. In the ESI positive mass spectrum of **1** a peak with an abundance of 100% is observed centered around m/z = 743, corresponding to $[LNi_2(OOCCH_3)]^+$, with the expected isotope pattern. The EI mass spectrum does not provide much useful information regarding the tetranuclear nature of **2**. It exhibits signals around m/z = 714−720 (100%) with the expected isotope pattern for a dinickel compound, clearly indicating the presence of $[LNi_2(OCH_3)]^+$ in the gas phase.

The electronic spectra of **1** and **2** show intense π-π* transitions below 480 nm, attributable to the ligand, as judged by their high absorption coefficients and comparison with the spectrum of the ligand Additionally, there are three broad, weak transitions in the visible-near IR region at 779, 858 and 1284 nm for **1**, indicating that the nickel ions are in an octahedral environment in solution as well as in the solid state (X-ray structure). Interestingly only one broad absorption is observed in the range 800−1300 nm for **2**.

The reaction of copper perchlorate and the Schiff-base ligand afforded either **3** or **4**, depending on the solvent system, in relatively high yield. In the absence of protic solvents, complex **3**, a methoxy-bridged dicopper(II) species, is transformed easily into **4** — a μ_4-oxo-tetracopper(II) complex — in the presence of the solvent mixture CH_3CN/CH_2Cl_2 (Scheme 1) indicating the stability of **4**. Adventitious water in the solvent serves as a source of the μ_4-oxo ligand. Selected IR data for complexes **3** and **4** are given in the Exp. Sect. The sharp peaks in the solid state FTIR spectrum due to ν(OH) of the ligand LH_3 occur at $\tilde{\nu}$ = 3523, 3492 and 3348 cm^{-1}. These bands are missing in **3** and **4**, indicating that the phenol character of the ligand has been lost upon complexation. For **4** a sharp band of medium intensity at 510 cm^{-1} is associated with the $\nu_{Cu\text{-}O}$ vibration in the Cu_4O core. Support for this assignment is obtained by comparison with the vibrational spectrum of **3**, which exhibits, similar to that for **4**, two sharp bands of medium intensity at 564 and 539 cm^{-1} attributable to ν(Cu−O) vibrations for bonds to the phenolate groups. These three bands are missing in the spectrum of the free ligand. In the

EI mass spectrum of **3** a molecular peak at $m/z = 724$, with an abundance of 100%, corresponding to the $LCu_2(OCH_3)$ species is observed. Additionally, a clear indication of the presence of THF in **3** is found at $m/z = 72$. Mass spectrometry in the EI mode has been proved to be very useful for **4**, for which the molecular peak at $m/z = 1404$, with the expected isotope pattern, confirms the presence of $[L_2Cu_4(O)]$. The electronic spectra of **3** and **4** in CH_2Cl_2 display four intense bands in the 600−200 nm region attributed to the Schiff-base ligand.

Single Crystal X-ray Diffraction Studies

Molecular Structure of 1

The structure of **1** (Figure 1, Table 1) shows the formation of a dinickel(II) complex with a bridging urea through

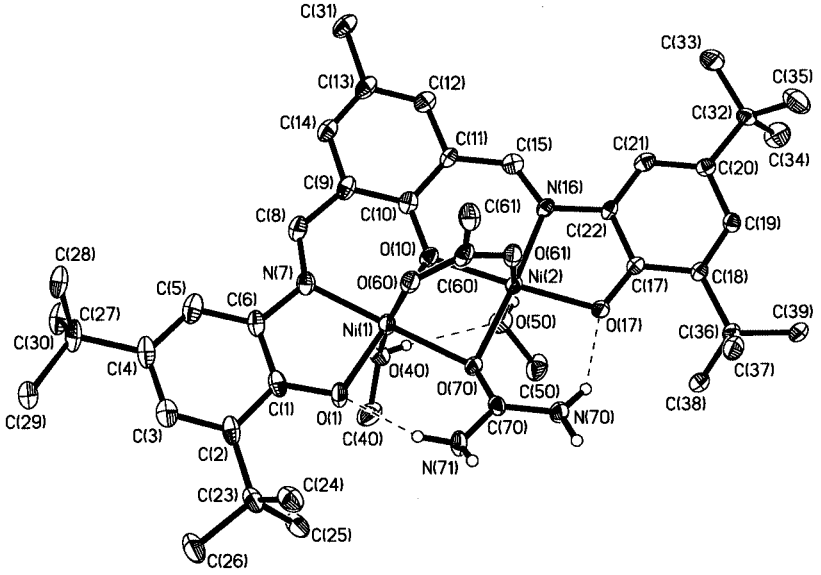

Figure 1. An ORTEP drawing of the neutral molecule **1**, $[LNi^{II}_2(NH_2CONH_2)(OOCCH_3)(CH_3OH)_2]\cdot 4.5CH_3OH$

Table 1. Crystallographic data for $[LNi^{II}_2(NH_2CONH)_2(O_2CMe)(MeOH)_2]\cdot 4.5MeOH$ (**1**), $[(LH)_2Ni^{II}_4(OMe)_2(O_2CMe)_2(MeOH)_2]\cdot 3CH_2Cl_2$ (**2**) and $[L_2Cu^{II}_4(\mu_4\text{-}O)\cdot 3.3CH_2Cl_2\cdot 0.7CH_3CN$ (**4**)

	Ni^{II}_2 (urea) **1**	Ni^{II}_4 **2**	$Cu^{II}_4(\mu_4\text{-}O)$ **4**
Empirical formula	$C_{42}H_{62}N_4Ni_2O_8\cdot 4.5CH_3OH$	$C_{82}H_{116}N_4Ni_4O_{14}\cdot 3CH_2Cl_2$	$C_{74}H_{94}Cu_4N_4O_7\cdot 3.3CH_2Cl_2\cdot 0.7CH_3CN$
Molecular weight	1012.57	1871.41	1715.56
Temperature	100(2) K	100(2) K	100(2) K
Wavelength (Mo-K_α)	0.71073 Å	0.71073 Å	0.71073 Å
Crystal System	Triclinic	Triclinic	Triclinic
Space group	$P\bar{1}$	$P\bar{1}$	$P\bar{1}$
Unit cell dimensions	$a = 12.099(2)$ Å	$a = 19.9102(12)$ Å	$a = 16.4678(9)$ Å
	$b = 12.128(2)$ Å	$b = 21.545(2)$ Å	$b = 17.2675(12)$ Å
	$c = 18.800(3)$ Å	$c = 22.076(2)$ Å	$c = 17.3208(12)$ Å
	$\alpha = 95.90(2)°$	$\alpha = 80.45(2)°$	$\alpha = 106.03(1)°$
	$\beta = 104.16(2)°$	$\beta = 80.88(2)°$	$\beta = 112.14(1)°$
	$\gamma = 91.48(2)°$	$\gamma = 83.43(2)°$	$\gamma = 102.71(1)°$
Volume (Å^3); Z	2656.9(8); 2	9182.7(13); 4	4083.9(5); 2
Density (calc.) Mg/m^3	1.266	1.354	1.395
Absorp. coeff. (mm^{-1})	0.769	1.043	1.298
$F(000)$	1086	3944	1785
Crystal size (mm)	0.20 × 0.19 × 0.10	0.18 × 0.10 × 0.09	0.33 × 0.24 × 0.15
θ range for data collect.	1.69 to 23.27°	3.13 to 22.50°	2.87 to 30.0°
Reflections collected	18237	57320	49175
Independent reflect.	7534 [R(int.) = 0.1014]	23751 [R(int.) = 0.0845]	23491 [R(int.) = 0.0452]
Absorpt. correction	Gaussian, face indexed	Gaussian, face indexed	not measured
Data/restraints/param.	7524/25/672	23751/112/2033	23356/166/964
Goodness-of-fit on F^2	0.877	1.051	1.019
Final R indices [$I > 2\sigma(I)$]	$R_1 = 0.0508$	$R_1 = 0.0837$	$R_1 = 0.0569$
	$wR_2 = 0.0971$	$wR_2 = 0.1851$	$wR_2 = 0.1434$
R indices (all data)	$R_1 = 0.1113$	$R_1 = 0.1412$	$R_1 = 0.0803$
	$wR_2 = 0.1134$	$wR_2 = 0.2173$	$wR_2 = 0.1602$

the carbonyl oxygen. Ni(1) and Ni(2) are additionally bridged by a phenolate oxygen [O(10)] and an acetate ion. Each nickel is in a distorted octahedral NO_5 environment, and is equatorially bound to the NO_3 donor set [Ni−N: av. 1.975 Å; Ni−O: av. 2.01 Å], with axial interactions to a carboxylic *O*-donor of a bridging $MeCO_2^-$ group [Ni−O: av. 2.09 Å] and a methanol *O*-donor [Ni−O: 2.165, 2.159 Å] trans to the $MeCO_2^-$ group. The hydrogen atoms of the hydroxy group in MeOH and the urea molecules were located from a difference map and are shown as circles of arbitrary radii in Figure 1. The hydrogen atoms on the NH_2 groups of urea enter into hydrogen bonding with the phenolate oxygens O(1) and O(17), with O(1)···N(71) and O(17)···N(70) distances of 2.784 and 2.813 Å, respectively, thus making urea presumably not susceptible to alcoholysis (see later). The intramolecular hydrogen bonds between the methanol molecules *cis*-ligated to two different nickel(II) ions [O(40)···O(50) 2.928 Å] are shown as dotted lines. The Ni(1)···Ni(2) distance of 2.966(1) Å in **2** is significantly shorter than those observed in comparable complexes.[14−15] The bridging Ni−O(urea) distances [2.080(3) and 2.065(3) Å] are significantly shorter than those in the only other single-atom *O*-bridged urea compound [Ni−O(urea): 2.158(3) Å].[15] The Ni−O(urea) bond lengths for compounds containing non-bridging urea lie within the range 2.05−2.13 Å.[14] The Ni(1)−O(70)−Ni(2) angle at the bridging urea is 91.4(1)°, whereas the phenoxide bridging angle Ni(1)−O(10)−Ni(2) is significantly greater [97.1(2)°].

Table 2. Selected bond lengths (Å) and angles (deg) for $[LNi^{II}_2(NH_2CONH_2)(OOCCH_3)(CH_3OH)_2]\cdot 4.5CH_3OH$ (**1**)

Ni(1)−O(1)	1.954(3)	O(1)−Ni(1)−N(7)	84.7(2)
Ni(1)−N(7)	1.971(4)	O(1)−Ni(1)−O(10)	175.4(2)
Ni(1)−O(10)	1.971(3)	N(7)−Ni(1)−O(10)	93.2(2)
Ni(1)−O(70)	2.080(3)	O(1)−Ni(1)−O(70)	97.52(13)
Ni(1)−O(60)	2.089(4)	N(7)−Ni(1)−O(70)	176.4(2)
Ni(1)−O(40)	2.165(4)	O(10)−Ni(1)−O(70)	84.38(13)
Ni(1)−Ni(2)	2.9656(11)	O(1)−Ni(1)−O(60)	95.39(14)
Ni(2)−O(17)	1.967(3)	N(7)−Ni(1)−O(60)	93.0(2)
Ni(2)−N(16)	1.978(4)	O(10)−Ni(1)−O(60)	88.84(14)
Ni(2)−O(10)	1.986(3)	O(70)−Ni(1)−O(60)	89.59(14)
Ni(2)−O(70)	2.065(3)	O(1)−Ni(1)−O(40)	94.6(2)
Ni(2)−O(61)	2.088(4)	N(7)−Ni(1)−O(40)	92.0(2)
Ni(2)−O(50)	2.159(4)	O(10)−Ni(1)−O(40)	81.33(14)
		O(70)−Ni(1)−O(40)	85.09(14)
		O(60)−Ni(1)−O(40)	169.22(13)
O(17)−Ni(2)−N(16)	84.6(2)	O(70)−C(70)	1.285(6)
O(17)−Ni(2)−O(10)	174.54(14)	N(70)−C(70)	1.323(7)
N(16)−Ni(2)−O(10)	91.6(2)	N(71)−C(70)	1.312(6)
O(17)−Ni(2)−O(70)	99.33(13)	Ni(1)···Ni(2)	2.966(1)
N(16)−Ni(2)−O(70)	175.7(2)		
O(10)−Ni(2)−O(70)	84.39(13)		
O(17)−Ni(2)−O(61)	94.20(14)		
N(16)−Ni(2)−O(61)	94.2(2)		
O(10)−Ni(2)−O(61)	89.96(13)		
O(70)−Ni(2)−O(61)	87.25(14)		
O(17)−Ni(2)−O(50)	92.8(2)		
N(16)−Ni(2)−O(50)	95.1(2)		
O(10)−Ni(2)−O(50)	83.7(2)		
O(70)−Ni(2)−O(50)	83.08(14)		
O(61)−Ni(2)−O(50)	168.89(13)		

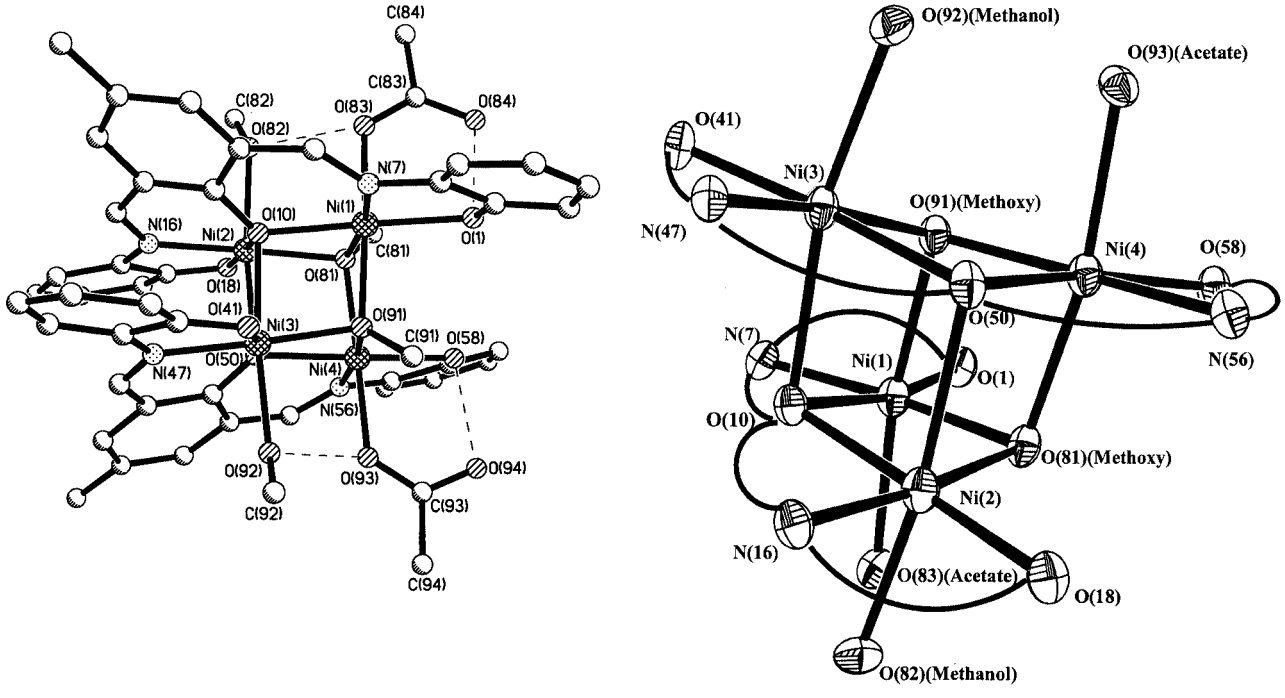

Figure 2. (a) Molecular structure of **2**, $[(LH)_2Ni^{II}_4(OCH_3)_2(OOCCH_3)_2(CH_3OH)_2]\cdot 3CH_2Cl_2$; (b) a view of **2** highlighting the Ni_4O_4 cubane core; the pentadentate ligand L is denoted only by the donor atoms joined by the curved lines

Relevant bond lengths and angles are summarized in Table 2.

Molecular Structure of 2

The crystal structure of **2** is shown in Figure 2, with selected bond lengths and angles provided in Table 3. The molecule is based on a roughly cubic Ni_4O_4 [16] unit, consisting of two interpenetrating tetrahedra, one of four nickel atoms and one of four μ_3-oxygen atoms originating from the cresol phenolate [O(10), O(50)] part of the ancillary ligand L and methoxide groups [O(81), O(91)]. Each Ni^{II} is in a distorted octahedral environment with an NO_5 donor set. For Ni(1) and Ni(4) a peripheral ligation is provided by a monodentate acetate ion, whereas for Ni(2) and Ni(3) a methanol molecule [O(82) and O(92), respectively] completes the sixth coordination position. The ancillary Schiff-base ligands are present in their monoprotonated form HL and are protonated at O(1) and O(58), forming hydrogen bonds with O(84) and O(94) of the acetate ions, respectively [O(1)···O(84): 2.426 Å; O(58)···O(94): 2.449 Å]. Although it was not possible to locate all the hydrogen atoms in the structure, the intramolecular contacts between the oxygen atoms of the methanol molecules [O(82) and O(92)] and the oxygen atoms of the acetate groups [O(83) and O(93), respectively] of 2.657 Å and 2.684 Å, can be interpreted as hydrogen bonds. The Ni−O−Ni angles vary between 94.4(2) and 102.2(3)°. The Ni···Ni distances on different cubic faces are also different, the shortest being Ni(1)···Ni(2) (3.047 Å) and the longest Ni(2)···Ni(3) (3.227 Å). Average Ni−N and Ni−O bond lengths of 1.99 and 2.10 Å, respectively, lie well within the range of reported values for the corresponding bond lengths of the tetranuclear cubane-like Ni^{II}.[16] No substantial differences in bond lengths and angles are found between the two crystallographically independent molecules.

Table 3. Selected bond lengths (Å) and angles (deg) for $[(LH)_2Ni^{II}_4(OCH_3)_2(OOC{\cdot}CH_3)_2(CH_3OH)_2]{\cdot}3CH_2Cl_2$ (**2**)

Ni(1)−N(7)	1.988(7)	N(7)−Ni(1)−O(91)	100.1(3)
Ni(1)−O(91)	2.050(6)	N(7)−Ni(1)−O(81)	170.6(3)
Ni(1)−O(81)	2.052(6)	O(91)−Ni(1)−O(81)	80.9(2)
Ni(1)−O(10)	2.081(6)	N(7)−Ni81)−O(10)	88.5(3)
Ni(1)−O(1)	2.089(6)	O(91)−Ni(1)−O(10)	82.3(2)
Ni(1)−O(83)	2.112(6)	O(81)−Ni(1)−O(10)	82.4(2)
Ni(2)−O(18)	1.970(6)	N(7)−Ni(1)−O(1)	80.9(3)
Ni(2)−N(16)	1.984(7)	O(91)−Ni(1)−O(1)	93.7(2)
Ni(2)−O(81)	2.024(6)	O(81)−Ni(1)−O(1)	108.4(2)
Ni(2)−O(10)	2.049(6)	O(10)−Ni(1)−O(1)	167.9(2)
Ni(2)−O(82)	2.123(6)	N(7)−Ni(1)−O(83)	90.5(3)
Ni(2)−O(50)	2.229(6)	O(91)−Ni(1)−O(83)	169.3(2)
Ni(3)−O(41)	1.970(6)	O(81)−Ni(1)−O(83)	88.4(2)
Ni(3)−N(47)	1.994(7)	O(10)−Ni(1)−O(83)	96.4(2)
Ni(3)−O(91)	2.052(6)	O(1)−Ni(1)−O(83)	89.6(2)
Ni(3)−O(50)	2.054(6)	O(18)−Ni(2)−N(16)	83.8(3)
Ni(3)−O(92)	2.109(6)	O(18)−Ni(2)−O(81)	101.3(2)
Ni(3)−O(10)	2.219(6)	N(16)−Ni(2)−O(81)	174.3(3)
Ni(4)−N(56)	1.979(7)	O(18)−Ni(2)−O(10)	174.3(2)
Ni(4)−O(91)	2.042(6)	N(16)−Ni(2)−O(10)	90.9(3)
Ni(4)−O(81)	2.055(6)	O(81)−Ni(2)−O(10)	83.9(2)
Ni(4)−O(50)	2.069(6)	O(18)−Ni(2)−O(82)	96.4(3)
Ni(4)−O(93)	2.092(7)	N(16)−Ni(2)−O(82)	88.6(3)
Ni(4)−O(58)	2.126(6)	O(81)−Ni(2)−O(82)	93.2(2)
		O(10)−Ni(2)−O(82)	85.5(2)
O(41)−Ni(3)−N(47)	83.5(3)	O(18)−Ni(2)−O(50)	96.9(2)
O(41)−Ni(3)−O(91)	103.7(2)	N(16)−Ni(2)−O(50)	96.9(3)
N(47)−Ni(3)−O(91)	172.1(3)	O(81)−Ni(2)−O(50)	80.2(2)
O(41)−Ni(3)−O(50)	173.7(2)	O(10)−Ni(2)−O(50)	81.8(2)
N(47)−Ni(3)−O(50)	90.6(3)	O(82)−Ni(2)−O(50)	166.1(2)
O(91)−Ni(3)−O(50)	82.2(2)		
O(41)−Ni(3)−O(92)	94.5(3)	Ni(2)−O(10)−Ni(3)	98.1(2)
N(47)−Ni(3)−O(92)	89.5(3)	Ni(1)−O(10)−Ni(3)	95.8(2)
O(91)−Ni(3)−O(92)	93.3(2)	Ni(2)−O(81)−Ni(1)	96.8(2)
O(50)−Ni(3)−O(92)	87.5(2)	Ni(2)−O(81)−Ni(4)	101.3(2)
O(41)−Ni(3)−O(10)	96.8(2)	Ni(1)−O(81)−Ni(4)	98.1(3)
N(47)−Ni(3)−O(10)	97.0(3)	Ni(4)−O(91)−Ni(1)	98.6(3)
O(91)−Ni(3)−O(10)	78.9(2)	Ni(4)−O(91)−Ni(3)	97.5(2)
O(50)−Ni(3)−O(10)	81.9(2)	Ni(1)−O(91)−Ni(3)	102.2(3)
O(92)−Ni(3)−O(10)	167.6(2)	Ni(3)−O(50)−Ni(4)	96.5(2)
N(56)−Ni(4)−O(91)	171.3(3)	Ni(3)−O(50)−Ni(2)	97.7(2)
N(56)−Ni(4)−O(81)	99.8(3)	Ni(4)−O(50)−Ni(2)	94.4(2)
O(91)−Ni(4)−O(81)	81.0(2)	Ni(2)−O(10)−Ni(1)	95.1(2)
N(56)−Ni(4)−O(50)	89.4(3)		
O(91)−Ni(4)−O(50)	82.0(2)	Ni(1)···Ni(2)	3.047
O(81)−Ni(4)−O(50)	83.4(2)	Ni(3)···Ni(4)	3.077
N(56)−Ni(4)−O(93)	89.8(3)	Ni(1)···Ni(3)	3.191
		Ni(2)···Ni(4)	3.155
O(91)−Ni(4)−O(93)	89.0(2)	Ni(1)···Ni(4)	3.102
O(81)−Ni(4)−O(93)	169.9(2)	Ni(2)···Ni(3)	3.227
O(50)−Ni(4)−O(93)	93.7(2)		
N(56)−Ni(4)−O(58)	80.2(3)		
O(91)−Ni(4)−O(58)	108.5(2)		
O(81)−Ni(4)−O(58)	94.0(2)		
O(50)−Ni(4)−O(58)	168.7(2)		
O(93)−Ni(4)−O(58)	90.7(2)		

Molecular Structure of 3

Although the analytical and spectroscopic data show the presence of a dinuclear Cu_2 core as the smallest unit in **3**, an X-ray analysis was undertaken to remove any doubts regarding the connectivity. Unfortunately, crystals of **3**

Table 4. Selected bond lengths (Å) and angles (deg) for $[LCu^{II}_2(OCH_3)(THF)_2]{\cdot}2THF$ (**3**)

Cu(1)−O(1)	1.899(6)	Cu(2)−O(17)	1.880(7)
Cu(1)−O(40)	1.911(6)	Cu(2)−O(40)	1.905(6)
Cu(1)−N(7)	1.915(8)	Cu(2)−N(16)	1.931(8)
Cu(1)−O(10)	1.948(6)	Cu(2)−O(10)	1.952(7)
Cu(1)−O(60)		Cu(2)−O(50)	
Cu(1)−O(10)−Cu(2)	99.38(31)		
Cu(1)−O(40)−Cu(2)	102.43(31)		
O(1)−Cu(1)−O(10)	173.32(27)		
O(40)−Cu(1)−N(7)	170.28(28)		
O(1)−Cu(1)−O(40)	100.83(26)		
O(1)−Cu(1)−N(7)	86.78(29)		
O(40)−Cu(1)−O(10)	78.49(27)		
O(10)−Cu(1)−N(7)	93.25(30)		
O(40)−Cu(2)−O(10)	78.55(27)		
O(40)−Cu(2)−N(16)	167.77(30)		
O(40)−Cu(2)−O(17)	101.62(29)		
O(10)−Cu(2)−N(16)	92.48(33)		
O(10)−Cu(2)−O(17)	172.80(28)		
N(16)−Cu(2)−O(17)	86.24(34)		
Cu(1)···Cu(2)	2.974(2)		

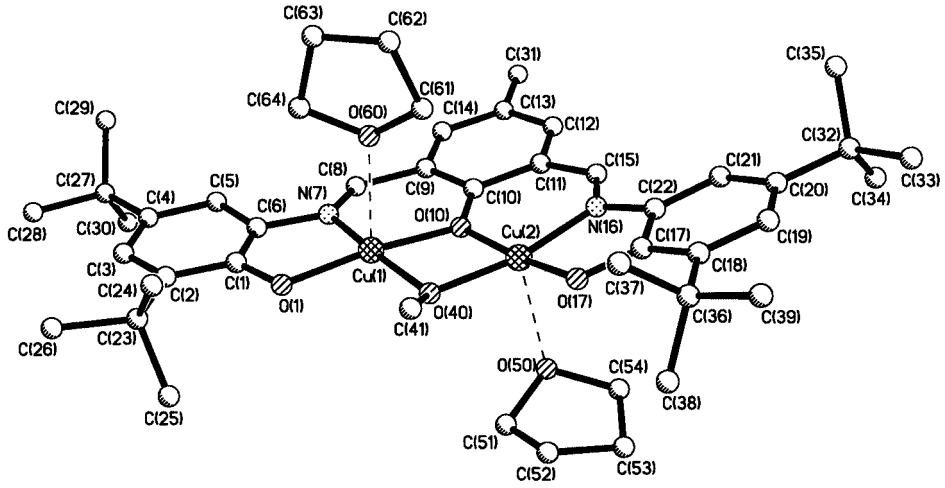

Figure 3. A perspective view of the neutral complex $[LCu_2(OCH_3)(THF)_2]$ **3**

$[C_{46}H_{66}N_2O_6Cu_2 \cdot 2THF$, monoclinic, space group $P2_1/n$, $a = 11.7459(12)$, $b = 30.236(3)$, $c = 15.640(2)$ Å, $\beta = 110.19(3)°$, $V = 5213.2$ Å^3, $T = 100(2)$ K, final $R = 0.092$ for 5150 independent reflections] diffract X-rays very weakly. In spite of the high R factor and large standard deviations, the crystal structure analysis of **3** confirmed its dinuclear structure. Because of its unacceptable quality, we are refraining from publishing the crystal data in detail. Selected bond lengths and angles are given in Table 4. The crystal structure reveals that the copper atoms are doubly bridged by the phenoxo and by a methoxide group (Figure 3). The pentacoordination of copper atoms is achieved by a tetrahydrofuran oxygen with Cu(1)−O(60) and Cu(2)−O(50) distances of 2.444 Å and 2.566 Å, respectively, which are oriented *trans* to each other in the dicopper complex. The coordination polyhedron for the copper centers is a distorted square pyramid with O(1)N(7)O(10)O(40) for Cu(1) and O(10)N(16)O(17)O(40) for Cu(2) forming the equatorial planes, where Cu(1) and Cu(2) are located 0.102 Å and 0.134 Å, respectively, out of the equatorial planes. The ring Cu(1)O(10)Cu(2)O(40) is not planar, the dihedral angle being 12.7°. The distances Cu−N and Cu−O are in the ranges reported for comparable complexes.[17]

Molecular Structure of 4

The molecular structure of **4** is shown in Figure 4. Selected interatomic distances and bond angles are listed in Table 5. Compound **4** consists of four copper(II) ions

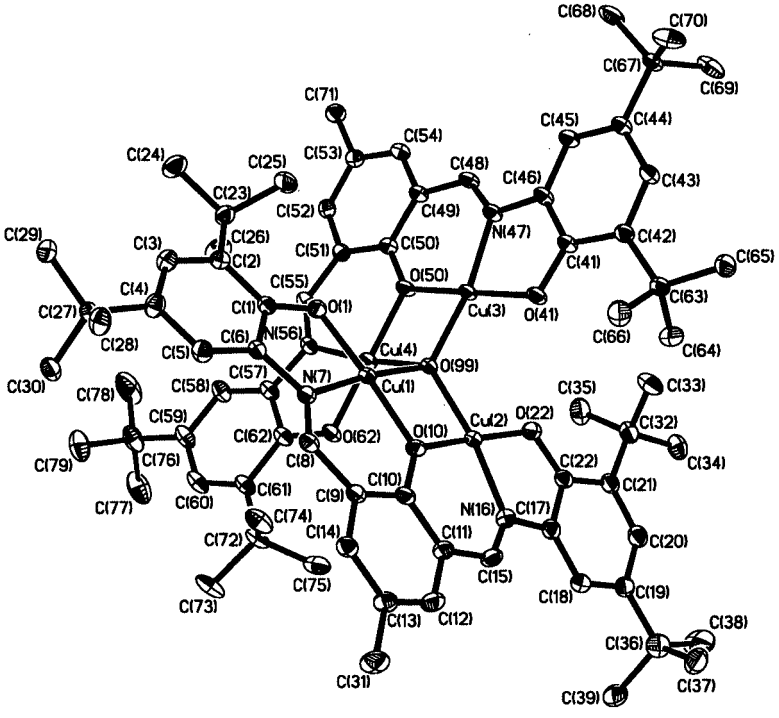

Figure 4. Molecular structure of $[L_2Cu_4(\mu_4\text{-}O)]$ **4**

Table 5. Selected interatomic distances (Å) and angles (deg) for $[L_2Cu^{II}(\mu_4\text{-}O)]\cdot 3.3CH_2Cl_2\cdot 0.7CH_3CN$ (**4**)

Cu(1)−O(1)	1.903(2)	O(1)−Cu(1)−N(7)	86.44(10)
Cu(1)−N(7)	1.919(3)	O(1)−Cu(1)−O(10)	175.87(9)
Cu(1)−O(10	1.925(2)	N(7)−Cu(1)−O(10)	93.86(10)
Cu(1)−O(99)	1.953(2)	O(1)−Cu(1)−O(99)	99.59(9)
Cu(2)−O(22)	1.897(2)	N(7)−Cu(1)−O(99)	173.77(10)
Cu(2)−O(99)	1.915(2)	O(10)−Cu(1)−O(99)	80.02(9)
Cu(2)−N(16)	1.927(3)	O(1)−Cu(1)−Cu(4)	71.26(7)
Cu(2)−O(10)	1.956(2)	N(7)−Cu(1)−Cu(4)	137.58(7)
Cu(3)−O(41)	1.897(2)	O(10)−Cu(1)−Cu(4)	106.01(7)
Cu(3)−O(99)	1.915(2)	O(99)−Cu(1)−Cu(4)	44.71(6)
Cu(3)−N(47)	1.932(2)	O(1)−Cu(1)−Cu(2)	138.52(7)
Cu(3)−O(50)	1.950(2)	N(7)−Cu(1)−Cu(2)	134.27(8)
Cu(4)−O(62)	1.891(2)	O(10)−Cu(1)−Cu(2)	40.64(6)
Cu(4)−N(56)	1.916(3)	O(99)−Cu(1)−Cu(2)	39.53(6)
Cu(4)−O(50)	1.920(2)	Cu(4)−Cu(1)−Cu(2)	71.43(2)
Cu(4)−O(99)	1.942(2)	O(22)−Cu(2)−O(99)	102.40(9)
		O(22)−Cu(2)−N(16)	86.48(11)
Cu(2)−O(99)−Cu(3)	122.37(11)	O(99)−Cu(2)−N(16)	170.27(10)
Cu(2)−O(99)−Cu(4)	120.30(11)	O(22)−Cu(2)−O(10)	174.81(9)
Cu(3)−O(99)−Cu(4)	99.58(9)	O(99)−Cu(2)−O(10)	80.20(9)
Cu(2)−O(99)−Cu(1)	99.98(9)	N(16)−Cu(2)−O(10)	91.26(10)
Cu(3)−O(99)−Cu(1)	121.07(11)	O(22)−Cu(2)−Cu(1)	142.89(7)
Cu(4)−O(99)−Cu(1)	90.23(8)	O(99)−Cu(2)−Cu(1)	40.49(6)
Cu(4)−O(50)−Cu(3)	99.12(9)	N(16)−Cu(2)−Cu(1)	130.53(8)
Cu(1)−O(10)−Cu(2)	99.49(9)	O(10)−Cu(2)−Cu(1)	39.86(6)
		O(41)−Cu(3)−O(99)	101.94(9)
Cu(1)···Cu(4)	2.760(1)	O(41)−Cu(3)−N(47)	86.63(10)
Cu(1)···Cu(2)	2.963(1)	O(99)−Cu(3)−N(47)	169.95(10)
Cu(3)···Cu(4)	2.945(1)	O(41)−Cu(3)−O(50)	174.51(10)
Cu(1)···Cu(3)	3.368(1)	O(99)−Cu(3)−O(50)	80.61(9)
Cu(2)···Cu(4)	3.345(1)	N(47)−Cu(3)−O(50)	91.31(10)
Cu(2)···Cu(3)	3.356(1)	O(41)−Cu(3)−Cu(4)	142.25(6)
		O(99)−Cu(3)−Cu(4)	40.54(6)
		N(47)−Cu(3)−Cu(4)	131.12(8)
		O(50)−Cu(3)−Cu(4)	40.07(6)
		O(62)−Cu(4)−N(56)	87.16(10)
		O(62)−Cu(4)−N(50)	178.00(9)
		N(56)−Cu(4)−O(50)	94.35(10)
		O(62)−Cu(4)−O(99)	97.66(9)
		N(56)−Cu(4)−O(99)	172.05(10)
		O(50)−Cu(4)−O(99)	80.69(9)
		O(62)−Cu(4)−Cu(1)	131.72(8)
		N(56)−Cu(4)−Cu(1)	104.47(6)
		O(50)−Cu(4)−Cu(1)	45.06(6)
		O(99)−Cu(4)−Cu(1)	137.53(7)
		O(62)−Cu(4)−Cu(3)	134.87(8)
		N(56)−Cu(4)−Cu(3)	40.81(6)
		O(50)−Cu(4)−Cu(3)	39.88(6)
		O(99)−Cu(4)−Cu(3)	72.29(2)

bridged by a central μ_4-oxygen atom in an approximately tetrahedral environment. The phenolate oxygen atoms O(10) and O(50) of the cresol part of the ligand bridge two copper centers, resulting in very similar Cu(1)−O(10)−Cu(2) and Cu(3)−O(50)−Cu(4) angles of 99.49(9)° and 99.12(9)°, respectively. Each copper center is coordinated by three oxygen atoms and one nitrogen atom, with the bond lengths ranging from 1.891(2) to 1.953(2) Å. There are considerable deviations of the geometry of the copper center from the ideal square plane, as indicated by the basal plane angles (Table 5), although each CuO_3N portion is essentially planar. The dihedral angles between the Cu(1)/Cu(2) planes, and between the Cu(3)/Cu(4) planes are 8.5° and 3.2°, respectively. The two $Cu_2O_4N_2$ dinuclear units are nearly perpendicular, as evidenced by the dihedral angle of 75.2° between the Cu(1)O(10)Cu(2)O(99) and Cu(3)O(50)-Cu(4)O(99) planes.

The copper tetrahedron around the μ_4-oxygen O(99) is distorted, as the bond angles Cu−O(99)−Cu range from 122.37(1)° for Cu(2)−O(99)−Cu(3) to 90.23(8) for Cu(4)−O(99)−Cu(1), the smallest among the six angles at O(99). Perhaps as a consequence, the Cu(2)···Cu(3) distance of 3.356 Å is substantially longer than that of Cu(4)···Cu(1) (2.759 Å). The remaining Cu···Cu distances are Cu(1)···Cu(2) (2.963 Å), Cu(1)···Cu(3) (3.368 Å), Cu(2)···Cu(4) (3.345 Å) and Cu(3)···Cu(4) (2.945 Å). These differences can be explained by the steric forces of the chelating ligand L^{3-}, which contracts the Cu(1)−O(99)−Cu(4) angle with a concomitant expansion of the opposite angle Cu(2)−O(99)−Cu(3). Examples of tetranuclear copper(II) complexes with a μ_4-O kernel are abundant,[18−20] but all of them involve bridging ligands like halides or carboxylates between the edges of the tetrahedron. Compound **4** without any such bridging ligand is an exception. Figure 5 highlights the core structure for greater clarity and to emphasize the unique structure of the $Cu_4(\mu_4\text{-}O)$ unit present in **4**.

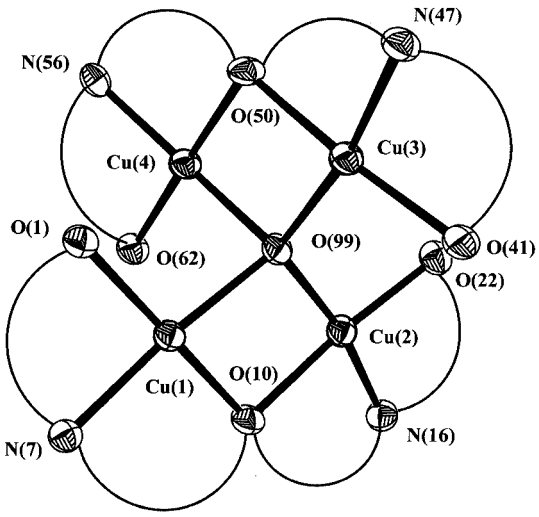

Figure 5. The atom connectivity in the core of complex **4**

Magnetic Susceptibility Studies

Magnetic susceptibility data for polycrystalline samples of complexes **1**−**4** were collected in the temperature range 2−290 K in an applied magnetic field of 1 T to characterize the nature and magnitude of the exchange interaction propagated by the bridging ligands. We use the Heisenberg spin-Hamiltonian in the form $H = -2JS_AS_B$ for an isotropic exchange coupling, with $S_{Ni} = 1$ for **1** and **2** and $S_{Cu} = 1/2$ for **3** and **4**. The experimental magnetic data were simulated using a least-squares fitting computer program[21] with a full-matrix diagonalization of exchange coupling, Zeeman splitting, and axial single-ion zero-field interactions [DS_z^2], if necessary. The susceptibility data were cor-

rected for diamagnetism (Pascal corrections), temperature-independent paramagnetism (TIP) and the presence of paramagnetic monomer impurities (P) in the following way: $\chi_{calc} = (1 - P)\chi + \chi_{TIP} + P\chi_{mono}$. The experimental data are displayed in Figure 6 as the effective magnetic moment (μ_{eff}) versus temperature (T). The solid lines in the figure represent the simulations.

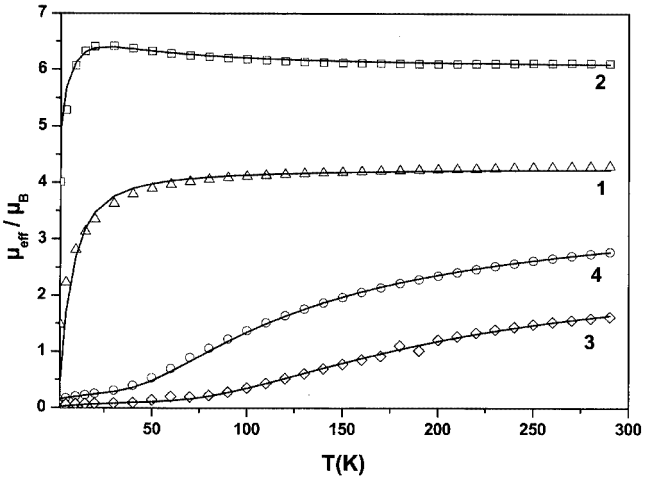

Figure 6. Plots of μ_{eff} vs. T for solid **1**, **2**, **3** and **4**; the solid lines represent the best fit of the data to the exchange coupling models

The magnetic moment μ_{eff}/molecule for **1** of 4.280 μ_B ($\chi_M \cdot T$ = 2.291 cm^3·K·mol^{-1}) at 290 K decreases monotonically with decreasing temperature until it reaches a value of 1.474 μ_B ($\chi_M \cdot T$ = 0.2717 cm^3·K·mol^{-1}) at 2 K; this temperature dependence of μ_{eff} is a clear indication of an antiferromagnetic exchange coupling between two paramagnetic centers Ni^{II} (S_{Ni} = 1) with a resulting diamagnetic ground state. Using only D (i.e. J = 0), a fit of poor quality with unusually large D was obtained and hence discarded. Attempts to fit the data using both D and J yield physically meaningless D values. For example, a good fit (not shown) was obtained with the following parameters: J = −2.6 cm^{-1}, D = +27.1 cm^{-1}, g = 2.13, P = 0.005. As the zero-field splitting D is unusually large for a six-coordinate Ni^{II} ion, this solution was also discarded. Finally, the solid line in Figure 6 represents the best fit with the following parameters: J = −3.5 cm^{-1}, $g_1 = g_2$ = 2.137, P = 0.005. The quality of the fit (Figure 6) is insensitive to D varying between 0 and 5 cm^{-1}.

For **2**, the effective magnetic moment of 6.08 μ_B ($\chi_M \cdot T$ = 4.629 cm^3·K·mol^{-1}) at 290 K increases monotonically with decreasing temperature reaching a broad maximum at 20−30 K with μ_{eff} = 6.39 μ_B ($\chi_M \cdot T$ = 5.1073 cm^3·K·mol^{-1}). Below 20 K, μ_{eff} starts to decrease reaching a value of 3.99 μ_B ($\chi_M \cdot T$ = 1.992 cm^3·K·mol^{-1}) at 2 K (Figure 6); it is clear that the magnetic properties of **2** are dominated by a ferromagnetic exchange interaction between four $^3A_2$ nickel(II) ions as propagated by bridging phenoxides and methoxides. The structural parameters of **2** strongly suggest a lower symmetry than T_d (idealized D_{2d}) for the molecule. The magnetic analyses were carried out using either a two-J or three-J model based on the diagram shown in Scheme 2.

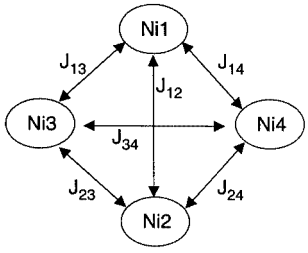

Scheme 2

The data were fit initially by using a higher symmetry model, i.e. $J_{12} = J_{34}$ and $J_{13} = J_{14} = J_{24} = J_{23}$, which yielded a good fit (not shown) with $J_{12} = J_{34}$ = +1.5 cm^{-1}, $J_{13} = J_{14} = J_{24} = J_{23}$ = +0.25 cm^{-1}, g = 2.133, D = 14.8 cm^{-1}. We discarded this solution as the zero-field splitting D is unusually large for a six-coordinate $^3A_2$ Ni^{II} ion.[22] We therefore fitted the data with three different exchange parameters, which also corroborate with three different types of faces present in the Ni_4O_4 cubane core of **2**. The best fit parameters are: $J_{12} = J_{34}$ = +0.47 cm^{-1}, $J_{13} = J_{24}$ = +4.25 cm^{-1}, $J_{14} = J_{23}$ = −1.45 cm^{-1}, g = 2.122 and D = 0 (fixed). The most important parameter in the magnetostructural correlation of the Ni_4O_4 cubane cores has been described in the literature[16] to be the averaged Ni−O−Ni angle of a cubane face. A ferromagnetic exchange interaction is observed when this angle is close to orthogonality. On the other hand, Ni−O−Ni angles in the vicinity of, and larger than, 99° lead to an antiferromagnetic interaction. Thus, the strongest ferromagnetic coupling, $J_{13} = J_{24}$ = +4.25 cm^{-1}, should be associated with the average Ni(1)−O−Ni(3) angle of 99.0°, which is not in agreement with the magnetostructural correlation reported in the literature.[16] This suggested that a better fitting model should be used. We therefore fitted the data by again using three different exchange parameters, but with the following constraints: J_{12}, J_{13} and $J_{14} = J_{24} = J_{23} = J_{34}$, as three different ranges of average Ni−O−Ni angles of 96°, 97−98° and 99° are present in **2**. The best fit obtained with the parameter set J_{12} = +8.0 cm^{-1}, $J_{14} = J_{24} = J_{23} = J_{34}$ = +0.9 cm^{-1}, J_{13} = −3.95 cm^{-1}, g = 2.120, D = 0 (fixed) is shown as a solid line in Figure 6. The differences and nature of the signs of the exchange parameters are in full agreement with the Ni−O−Ni angle correlation and support the three-J model used, which takes into account the reduced symmetry of the cubane core observed in the X-ray structure of **2**. Thus, these results for **2** predict a switch from ferromagnetic to antiferromagnetic coupling only for Ni−O−Ni angles above 98°.

Recently it has been demonstrated[16i] that the major contributor to the superexchange constants observed in $[Ni_4(OR)_4]^{4+}$ cubanes is the Ni−O−Ni angle. Accordingly, a linear correlation between J and the Ni−O−Ni angle has

been reported.[16i,16m] We have also plotted the observed J values for **2** and other structurally characterized $[Ni_4(OR)_4]^{4+}$ cubanes against average Ni−O−Ni angles (Figure 7). The solid line drawn as a guide for the eyes shows a fairly good correlation between J and these angles. This guide allows us to notice that the antiferromagnetic interactions ($-J$) fall fairly well on the correlated line with respect to Ni−O−Ni angles. In contrast, the positive J values scatter appreciably. This is not surprising considering the high tolerance attached in general to the positive J values (ferromagnetic interactions) evaluated through simulation of the susceptibility data.

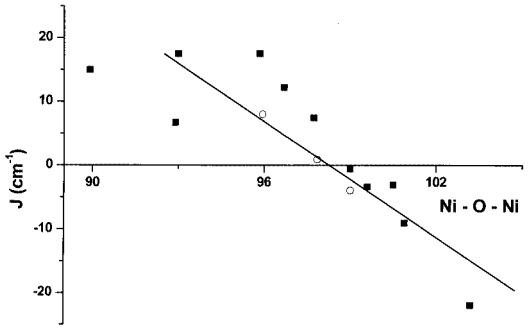

Figure 7. A plot of average Ni−O−Ni angles vs. the exchange interactions (J); closed circles are literature data and open circles are from this work; the solid line is drawn only as a guide

The non-zero magnetic moment of 3.99 μ_B at 2 K and the broad maximum with μ_{eff} = 6.39 μ_B at 20−30 K indicate that **2** has a complicated low-lying magnetic structure with a non-diamagnetic ground state smaller than the spin state of S_t = 4 expected for a ferromagnetically coupled tetranuclear nickel(II) moiety (S_{Ni} = 1). The ground state can be determined by examining the magnetization of the compound at low temperatures as a function of the applied magnetic fields. We have performed magnetization measurements at applied magnetic fields of 1, 4 and 7 T. The field-dependent magnetizations as a function of temperature, and their simulations, are depicted in Figure 8. It is clear from Figure 8 that the saturated magnetization value reaches a value of approximately 3.035 in the temperature range 2.0−2.8 K at the highest field of 7 T. The simulated parameters are: J_{12} = +8.0 cm^{-1}, J_{13} = −3.95 cm^{-1}, J_{14} = J_{24} = J_{23} = J_{34} = +0.60 cm^{-1}, g = 2.12, $|D|$ = 3.0 cm^{-1}. These values agree well with those from the susceptibility measurements. As J_{12}, J_{13} and D are of similar magnitude, it is not possible to calculate the ground state in the form of an S_t value; S is not a good quantum number to describe the ground state, but rather M_S.

Variable-temperature magnetic data for **3** exhibit a steady decrease of μ_{eff} from 1.634 μ_B (χ_M·T = 0.3338 cm^3·K·mol^{-1}) at 290 K to 0.049 μ_B (χ_M·T = 0.03 × 10^{-3} cm^3·K·mol^{-1}) at 2 K, which is indicative of very strong intramolecular antiferromagnetic coupling. The experimental data were simulated with the parameter set J = −192.1 cm^{-1}, g = 2.055, TIP = 30 × 10^{-6}, P = 0 and is shown in Figure 6. The major factor controlling the exchange interactions in hydroxy-, alkoxy- and phenoxy-bridged copper(II) is the Cu−O−Cu bridge angle.[20,23] The average Cu−O−Cu bridge angle of 100.9° for **3** would result in an approximate J value of −250 cm^{-1} according to the empirical equation reported in the literature and it deviates appreciably from the experimentally determined value of −192 cm^{-1} for **3**. A possible reason for the weak exchange coupling in **3** may be the deviation from co-planarity within the central Cu_2O_2 ring. It seems plausible that the methoxide ion, with shorter Cu(1)−O(40) (1.911 Å) and Cu(2)−O(40) (1.905 Å) distances and a larger Cu(1)−O(40)−Cu(2) angle (102.43°) than those with the phenoxide ion, provides a better pathway for antiferromagnetic exchange coupling.[17]

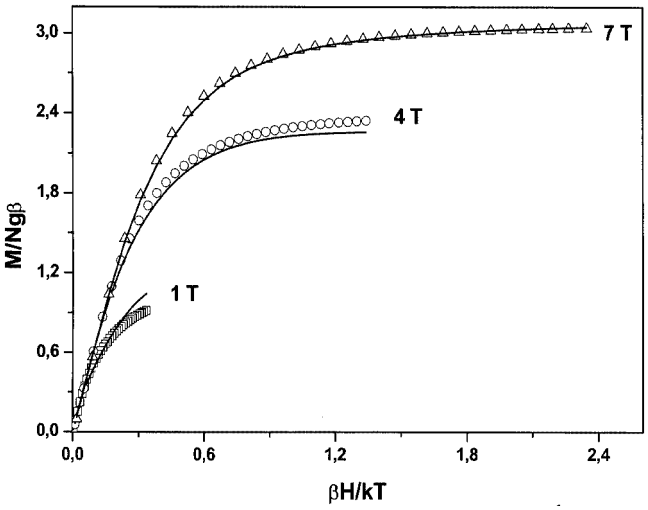

Figure 8. The field-dependent magnetizations of **2** as a function of temperature and their simulations; see text for the parameters

The effective magnetic moment μ_{eff}/molecule for **4** of 2.768 μ_B (χ_M·T = 0.9582 cm^3·K·mol^{-1}) at 290 K decreases monotonically with decreasing temperature until it reaches a value of 0.133 μ_B (χ_M·T = 0.0022 cm^3·K·mol^{-1}) at 2 K, indicating dominant antiferromagnetic interactions between four $^2B_2$ copper(II) ions; the data clearly show an S_t = 0 ground state for **4**.

Two different exchange pathways are possible for **4**: Cu-phenoxo-Cu and Cu-μ_4-oxo-Cu. Scheme 3 shows the connection of the copper centers through the phenoxo and the oxo groups.

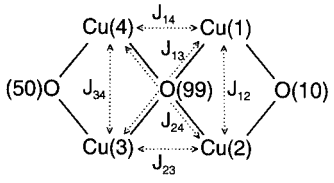

Scheme 3

As the Cu(3)/Cu(4) and Cu(2)/Cu(1) pairs are bridged by both phenoxo and oxo groups and the Cu(4)/Cu(1), Cu(2)/Cu(3), Cu(2)/Cu(4) and Cu(1)/Cu(3) pairs only through the oxo group, O(99), the experimental magnetic data were analyzed as a first approximation with a three-J model: J_{12} = J_{34}, J_{14} = J_{23} and J_{24} = J_{13}. In this model we have neglected the differences in the Cu−O−Cu angles. A very good fit

(not shown) was obtained with the following parameters: $J_{12} = J_{34} = -86.3$ cm^{-1}, $J_{14} = J_{23} = +40.8$ cm^{-1} and $J_{24} = J_{13} = -86.1$ cm^{-1}, $g = 1.976$, $D = 0$ (fixed), $P = 0.007$ and TIP $= 240 \times 10^{-6}$ which imply that the spin exchange is dominated by antiparallel coupling in **4**. The low g value and the positive coupling constants for both J_{14} and J_{23}, which represent the couplings between the copper centers with the angles Cu(4)−O(99)−Cu(1) (90.23°) and Cu(2)−O(99)−Cu(3) (122.37°), however, suggest that a better fitting model should be used. The data were consequently fitted to a more accurate model, again using a three-J model but with a different constraint based on the three ranges of Cu−O−Cu angles, 90.2, 99.12−99.98° and 120.30−122.37°. Thus, the following correlations between the six coupling constants depicted in Scheme 3 were used to fit the experimental data: $J_{12} = J_{34}$, $J_{23} = J_{24} = J_{13}$ and J_{14}. The fit shown in Figure 6 was obtained with $J_{12} = J_{34} = -122.3$ cm^{-1}, $J_{23} = J_{24} = J_{13} = -90.0$ cm^{-1} and $J_{14} = 0$, $g = 2.088$, $P = 0.003$, TIP $= 240 \times 10^{-6}$ and $D = 0$ (fixed). The susceptibility data consistent with this data set were found to be relatively insensitive to J_{14}, but very sensitive to J_{12} and J_{23}; J_{14} values lying in the range −20 to +20 cm^{-1} have no influence on the quality of simulation.

For copper(II) centers bridged by a ligand oxygen atom (oxo, hydroxo, alkoxo, phenoxo, etc.), a linear relationship of exchange coupling J with the average Cu−O−Cu angles in the Cu_2O_2 ring has been reported.[17,20,23] We note that although a J_{12} value of −122 cm^{-1} assigned to an angle of 99.5° does not deviate significantly from the reported linear relationship, the J_{23} value of −90.0 cm^{-1} deviates remarkably. This is not very surprising as the electronic structures of the μ-OR and μ_4-O groups are clearly different. J_{14} is nondeterminant for **4** within the measured temperature range 2−290 K.

Electrochemistry

Electrochemical voltammetric measurements (cyclic voltammetry, CV, and square-wave voltammetry, SQW) were performed with the complexes in CH_2Cl_2 solutions containing 0.1 M $TBAPF_6$. The copper(II) complexes **3** and **4** show very similar behavior. They exhibit an oxidation wave at +0.490 and +0.530 V, vs. Fc^+/Fc for **3** and **4**, respectively. The waves have a reversible appearance, although the peaks in CV and SQW are broad; the peak separation of the oxidative and reductive peaks in the CVs is relatively high (0.110 V even at low scan rates) and in SQW shoulders on the forward and reverse peaks are discernible. This leads us to assume that each of the complexes is oxidized at two different sites with redox potentials that differ somewhat in less than 0.1 V. Since a copper(II) oxidation is not feasible at such low potentials, we assign these redox processes to ligand-centered oxidation yielding two phenoxyl radicals in each complex.

The nickel(II) complexes **1** and **2** are oxidized in a similar potential range. There are waves at +0.470 (**1**) and +0.440 V (**2**), which are preceded by broad peaks (with shoulders in the SQW) at +0.270 V for **1** and +0.153 V for **2**. Additionally, with increasing scan rate the oxidation and re-reduction peaks in the CV were found to split into two components. We assign this more complex behavior to an involvement of the nickel(II) ion in the redox processes leading to radical through oxidation. Ligand-centered oxidation to a radical is inferred from the occurrence of oxidation processes at potentials that are similar, irrespective of the nature of the central metal ion. Involvement of central nickel ions in oxidation processes of radical complexes was documented earlier in detail,[24] including digital simulations of complex cyclic voltammograms.

Concluding Remarks

That single-atom *O*-bridging of urea in a dinuclear nickel(II) complex can be achieved with suitably designed ligands has been demonstrated by isolation of **1**. Unfortunately, **1** is not able to catalyze the ethanolysis of urea [conditions: 1 mmol of **1** and 50 mmol of urea in ethanol (10 mL) was refluxed at 80 °C for 14 hours, which was then worked up for the GC analysis] to form ethyl carbamate presumably because of the hydrogen bonding network involving urea in **1**, which is also maintained in solution. Due to the presence of a stable hydrogen-bonded structure in solution, there is no possibility of intramolecular OH^- delivery to the π*-orbital of urea, as has been proposed for the mechanism of action of urease.[13e,15] It is noteworthy that the bond lengths within the coordinated urea,[14] bridging or nonbridging, are very similar, in contrast to the compound which exhibits catalytic activity.[14g] In the latter compound two different C−N bond lengths — 1.348(4) and 1.303(4) Å — are observed within the coordinated urea.

Complex **2** contains the low-symmetry cubane core $[Ni_4(\mu_3\text{-phenoxide})_2(\mu_3\text{-methoxide})_2]^{4+}$ with differing Ni···Ni distances and Ni−O−Ni angles, resulting in three types of Ni_2O_2 faces. The observation of three discrete exchange parameters for **2** is consistent with the lower symmetry of the cubane than that of all others but one[16m] reported in the literature.[16] Figure 7, a plot of J vs. Ni−O−Ni angles for all structurally characterized Ni_4O_4 cubane cores, irrespective of their symmetry, exhibits a large variation of J values within a small span of Ni−O−Ni angles (90−103°). This figure also indicates that the symmetry of the cubane core has a profound effect on the magnetostructural correlation. It is likely that other structural parameters like Ni···Ni and Ni−O distances take the upper hand in the magnetostructural correlation for the low-symmetry cubane core. Thus, more such distorted cubane-type Ni^{II} complexes are needed to resolve this open question.

Complex **3** containing a (μ-methoxo)(μ-phenoxo)dicopper(II) unit belongs to a ubiquitous class of coordination complexes of copper(II). It is pertinent at this point to compare the magnetic properties of **3** with these related dicopper(II) complexes. Regardless of the coordination geometry of the copper centers — square planar, square pyramidal or trigonal bipyramidal — all complexes with a $Cu^{II}_2(\mu\text{-OPh})(\mu\text{-OCH}_3)$ core as in **3** are antiferromagnetic and show relatively moderate to strong spin coupling with values ran-

ging from −47 to −315 cm^{-1}. These observations extend over eight compounds,[17] in which it has been demonstrated that the $Cu(d_z^2)-O-Cu(d_z^2)$ pathway would yield weaker antiferromagnetic coupling than in related $Cu(d_{x^2-y^2})-O-Cu(d_{x^2-y^2})$ systems. The $-J$ values for six of these compounds lie in the range 150−224 cm^{-1}. The evaluated J value of −192 cm^{-1} for **1** falls at the upper end of the observed range and is in agreement with the paramagnetic copper(II) centers with $(d_{x^2-y^2})^1$ magnetic orbitals. The sum of the angles around the phenoxo-oxygen, O(10), is 357.7°, a planar phenoxo group capable of transmitting spin exchange effectively.

Complex **4**, $[L_2Cu_4(\mu_4\text{-}O)]$, is the first example of a (μ_4-oxo)tetranuclear copper(II) complex without any bridging ligand between the tetrahedral edges. In accordance with the three averaged Cu−O−Cu angles of 90°, 99.5° and 121.3°, a three-J model was used to analyze the magnetic data. It is interesting to note that an exchange coupling constant J_{14} corresponding to the Cu−O−Cu angle of 90° could not be evaluated.

Experimental Section

Materials and Physical Measurements: Reagent or analytical grade materials were obtained from commercial suppliers and used without further purification, except those for electrochemical measurements. Elemental analyses (C, H N) were performed by the Microanalytical Laboratory Dornis & Kolbe, Mülheim, Germany. Fourier transform infrared spectroscopy on KBr pellets was performed on a Perkin−Elmer 2000 FT-IR instrument. Electronic absorption spectra in solution were measured on a Perkin−Elmer Lambda 19 spectrophotometer. Magnetic susceptibilities of *powdered samples* were recorded on a SQUID magnetometer in the temperature range 2−295 K with an applied field of 1 T. Experimental susceptibility data were corrected for the underlying diamagnetism using Pascal's constants and for the TIP contributions. Cyclic voltammetric and coulometric measurements were performed on EG&G equipment (potentiostat/galvanostat model 273A). Mass spectra were obtained with either a Finnigan MAT 8200 (electron ionization, EIMS) or a MAT 95 (electrospray ESI-MS) instrument. A Bruker DRX 400 instrument was used for NMR spectra. Instrumental conditions for liquid chromatography are as follows: Shimadzu SPD-10 AV, Nucleodur-5-C_{18} Sel 220 column, UV-280 nm, eluent = CH_3CN (0.8 mL/min), room temperature, sample size 5 μL, recorder 0.5 cm/min.

H_3LtBu: 6-Amino-2,4-di-*tert*-butylphenol (4.4 g; 20 mmol) was added to a solution of 2,6-diformyl-4-methylphenol (1.6 g, 10 mmol) in methanol (70 mL), and the resulting solution was refluxed for 1 h, during which the color changed to deep red, and a yellow microcrystalline solid precipitated out. The solution was cooled, filtered and the solid was washed with cold methanol, and air-dried. Yield: 5.1 g (ca. 90%). The purity of the ligand was checked by liquid chromatography: Retention time of 13.2 min for the eluent CH_3CN with a rate of 0.8 mL/min. EI-MS: m/z = 570. ^1H NMR ($CDCl_3$): δ = 8.94, 7.26 (6 H, aromatic), 7.12 (2 H, −CH=N-), 2.38 (3 H, CH_3), 1.43 (18 H, tBu), 1.32 (18 H, tBu) ppm. IR (KBr disk): $\tilde{\nu}$ = 3523 cm^{-1}, 3492, 3348w, 2954, 2868s, 1625m, 1580m, 1482s, 1456s, 1361s, 1250s, 987s, 960s, 867m. *For the sake of simplicity the ligand is denoted by H_3L without the suffix tBu.* UV/Vis (CH_2Cl_2): λ_{max} (ε) = 270 nm (18600 $M^{-1}\cdot cm^{-1}$), 306 (17700), 401 (21800). UV/Vis [CH_2Cl_2 in the presence of eight equivalents of $(Bu_4N)OCH_3$]: λ_{max} (ε) = 300 nm (sh), 350 (sh), 496 (13900 $M^{-1}\cdot cm^{-1}$).

$[LNi^{II}_2(NH_2CONH_2)(OAc)(MeOH)_2]\cdot 4.5CH_3OH$ (1): $Ni(CH_3COO)_2\cdot 4H_2O$ (0.24 g; 1 mmol), CH_3COONa (0.16 g, 2 mmol) and urea (0.18 g, 3 mmol) were dissolved in methanol, and a solution of the ligand H_3L (0.28 g, 0.5 mmol) in dichloromethane (30 mL) was added. The resulting solution was refluxed for 15 min and filtered to remove any solid particles. The solution was allowed to evaporate slowly at ambient temperature to yield orange-red crystals. Yield: 0.24 g (60%). $C_{46.5}H_{80}N_4Ni_2O_{12.5}$ (1012.54): calcd. C 55.16, H 7.91, N 5.53, Ni 11.59; found C 55.8, H 7.4, N 6.0, Ni 11.7. MS-ESI pos. (in CH_2Cl_2): m/z = 743.5 $[M - (NH_2CONH_2)(CH_3OH)_2]^+$ (100%). EI-MS indicates the presence of both acetate and urea. IR (KBr disk): $\tilde{\nu}$ = 3586w cm^{-1}, 3382m, 3139m, 2950s, 2965m, 1670m, 1654m, 1568s, 1469s, 1444s, 1410s, 1250s, 1159m, 831m. UV/Vis (CH_2Cl_2): λ_{max} (ε) = 329 nm (14770 $M^{-1}\cdot cm^{-1}$), 464 (16900), 779 (19), 858 (27), 1284 (ca. 12).
Compound **1** can also be obtained from **2** by addition of urea and refluxing the resulting solution.

$[(LH)_2Ni^{II}_4(OMe)_2(OAc)_2(MeOH)_2]\cdot 3CH_2Cl_2$ (2): A solution of methanol (15 mL) containing $Ni(CH_3COO)_2\cdot 4H_2O$ (0.24 g, 1 mmol) and CH_3COONa (0.24 g, 3 mmol) was added to a solution of the ligand H_3L (0.28 g, 0.5 mmol) in dichloromethane (30 mL). The resulting solution was refluxed for 15 min, then cooled and filtered. On reduction of the volume of the filtrate orange-red microcrystals separated out. X-ray quality crystals were obtained by recrystallization from a dichloromethane/methanol mixture. Yield: 0.19 g (47%). $C_{82}H_{116}N_4Ni_4O_{14}$ (1616.60): calcd. C 60.92, H 7.23, N 3.47, Ni 14.52; found C 58.9, H 7.0, N 3.2, Ni 13.1. EI-MS: m/z = 714−720 (100) $[LNi_2(OCH_3)^+]$. IR (KBr disk): $\tilde{\nu}$ = 3440br cm^{-1}, 2955s, 1624s, 1552m, 1477s, 1446s, 1410s, 1259s, 1039s, 805m. UV/Vis (CH_2Cl_2): λ_{max} (ε): 331 nm (40300 $M^{-1}\cdot cm^{-1}$), 405 (32300), 474 (40600), 917 (26).

$[LCu^{II}_2(OCH_3)(THF)_2]\cdot 2THF$ (3): H_3L (0.29 g, 0.5 mmol), $Cu(ClO_4)_2\cdot 6H_2O$ (0.37 g, 1 mmol) and NEt_3 (0.3 mL) were added to a methanol/dichloromethane (1:3) solvent mixture, and the resultant solution refluxed for 0.5 h. The deep-red solution yielded an orange-red microcrystalline solid on slow evaporation of the solvent at ambient temperature. Yield: 0.13 g (70%). $C_{38}H_{50}Cu_2N_2O_4$ (725.92): calcd. C 62.87, H 6.94, N 3.86, Cu 17.51; found C 63.1, H 6.9, N 3.8, Cu 17.4. X-ray quality crystals were obtained by recrystallization with a THF/CH_3OH solvent mixture. EI-MS: m/z = 726 (100) $[LCu_2(OCH_3)]$; a clear indication of the presence of THF. IR (KBr disk): $\tilde{\nu}$ = 2954s cm^{-1}, 2867m, 2816w, 1597m, 1557m, 1474s, 1445s, 1256s, 1159s, 1077m, 830m. UV/Vis (CH_2Cl_2): λ_{max} (ε): 486 nm (17100 $M^{-1}\cdot cm^{-1}$).

$[L_2Cu^{II}_4(\mu_4\text{-}O)]\cdot 3.3CH_2Cl_2\cdot 0.7CH_3CN$ (4): A solution of the ligand H_3L (0.29 g; 0.5 mmol) $Cu(ClO_4)_2\cdot 6H_2O$ (0.37 g; 1 mmol) and NEt_3 (0.3 mL) in acetonitrile/dichloromethane (1:3) was refluxed for 0.5 h and then kept at room temperature to allow the separation of an orange-red microcrystalline substance, which was recrystallized from a CH_3CN/CH_2Cl_2 mixture to yield X-ray quality crystals. Yield: 0.21 g (60%). $C_{74}H_{94}Cu_4N_4O_7$ (1405.76): calcd. C 63.23, H 6.74, N 3.99, Cu 18.08; found C 62.4, H 6.9, N 4.0, Cu 17.8. EI-MS: m/z = 1402 $[M^+]$. IR (KBr disk): $\tilde{\nu}$ = 2952s cm^{-1}, 2904s, 2867m, 1593m, 1557m, 1467s, 1445s, 1409m, 1360m, 1317m, 1254s, 1200m, 1159s, 1077m, 829m, 564m, 539m, 510m. UV/Vis (CH_2Cl_2): λ_{max} (ε): 484 nm (35700 $M^{-1}\cdot cm^{-1}$), ca. 680sh (ca. 430).

Compound **4** can also be obtained by refluxing **3** in CH_3CN/CH_2Cl_2 for 0.5 h.

X-ray Crystallographic Data Collection and Refinement of the Structures: A single crystal of **1** (orange-red), **2** (red), **3** (orange-red) or **4** (orange-red) was coated with perfluoropolyether, mounted on a glass fiber and placed in a Kappa-CCD diffractometer equipped with a cold nitrogen stream at 100 K. Graphite-monochromated Mo-K_α radiation (λ = 0.71073 Å) was used. Crystallographic data of the compounds **1**, **2** and **4** are listed in Table 1. Cell constants were obtained from a least-squares fit of the diffraction angles of several thousand strong reflections. Intensity data were corrected for Lorentz and polarization effects. The data sets of **1** and **2** were corrected for absorption, whereas the intensities of **4** were left uncorrected. The Siemens ShelXTL software package (G. M. Sheldrick, Universität Göttingen) was used for solution, refinement and artwork of the structures; the neutral atom scattering factors of the program were used. All structures were solved and refined by direct methods and difference-Fourier techniques. Non-hydrogen atoms were refined anisotropically, and hydrogen atoms were placed at calculated positions and refined as riding atoms with isotropic displacement parameters.

CCDC-191305 (**1**), -191306 (**2**), and -191307 (**4**) contain the supplementary crystallographic data for this paper. These data can be obtained free of charge at www.ccdc.cam.ac.uk/conts/retrieving.html [or from the Cambridge Crystallographic Data Centre, 12, Union Road, Cambridge CB2 1EZ, UK; Fax: (internat.) +44-1223/336-033; E-mail: deposit@ccdc.cam.ac.uk].

Acknowledgments

Financial support from the DFG (Grant: Priority program Ch111/2−1), the Max-Planck Society and Fonds der Chemischen Industrie is gratefully acknowledged. Thanks are due to Mrs. H. Schucht, Mrs. P. Höfer and Mr. A. Göbels for skilful technical assistance.

[1] For selected examples see: [1a] *Bioinorganic Chemistry of Copper* (Eds.: K. D. Karlin, Z. Tyeklar), Chapman & Hall, New York **1993**. [1b] *Manganese Redox Enzymes* (Ed.: V. L. Pecoraro), VCH Publishers, Weinheim **1992**. [1c] *Multicopper Oxidases* (Ed.: A. Messerschmidt), World Scientific, Singapore **1977**. [1d] T. N. Sorrell, *Tetrahedron* **1989**, *40*, 3. [1e] N. Kitajima, W. B. Tolman, *Progr, Inorg. Chem.* **1995**, *43*, 419. [1f] J. Du Bois, T. J. Mizoguchi, S. J. Lippard, *Coord. Chem. Rev.* **2000**, *200−202*, 443. [1g] V. Mahadevan, R. J. M. Klein Gebbink, T. D. P. Stack, *Curr. Opin. Chem. Biol.* **2000**, *4*, 228. [1h] L. Que, Jr., W. Tolman, *Angew. Chem.* **2002**, *114*, 1160; *Angew. Chem. Int. Ed.* **2002**, *41*, 1114.

[2] See for example: "*Journal of Solid State Chemistry''*, Vol. 159, No. 2, July 2001 − a tribute to Olivier Kahn.

[3] C. Desplanches, E. Ruiz, A. Rodriguez-Fortea, S. Alvarez, *J. Am. Chem. Soc.* **2000**, *124*, 5197 and references therein.

[4] [4a] R. Robson, *J. Inorg. Nucl. Chem. Lett.* **1970**, *6*, 125. [4b] R. Robson, *Aust. J. Chem.* **1970**, *23*, 2217. [4c] A. M. Bond, M. Haga, I. S. Creece, R. Robson, J. C. Wilson, *Inorg. Chem.* **1988**, *27*, 712. [4d] A. M. Bond, M. Haga, I. S. Creece, R. Robson, J. C. Wilson, *Inorg. Chem.* **1989**, *28*, 559.

[5] H. Okawa, H. Furutachi, D. E. Fenton, *Coord. Chem. Rev.* **1998**, *174*, 51 and references therein.

[6] [6a] C. N. Verani, T. Weyhermüller, E. Rentschler, E. Bill, P. Chaudhuri, *Chem. Commun.* **1998**, 2475. [6b] C. N. Verani, E. Rentschler, T. Weyhermüller, E. Bill, P. Chaudhuri, *J. Chem. Soc., Dalton Trans.* **2000**, 4263.

[7] C. Krebs, M. Winter, T. Weyhermüller, E. Bill, K. Wieghardt, P. Chaudhuri, *J. Chem. Soc., Chem. Commun.* **1995**, 1913.

[8] [8a] *Chem. Rev.* **1996**, *96*, No. 7. Guest Editors, R. H. Holm, E. I. Solomon. [8b] *Metal Ions in Biological Systems* (Eds.: H. Sigel, A. Sigel), Marcel-Dekker, New York, 1994, Vol. 30. [8c] G. T. Babcock, M. Espe, C. Hoganson, N. Lydakis-Simantiris, J. McCracken, W. Shi, S. Styring, C. Tommas, K. Warncke, *Acta Chem. Scand.* **1997**, *51*, 533. [8d] M. M. Fontecave, J. L. Pierre, *Bull. Soc. Chim. Fr.* **1996**, *133*, 653. [8e] D. P. Goldberg, S. J. Lippard, *Adv. Chem. Ser.* **1995**, *246*, 59. [8f] J. Stubbe, W. A. van der Donk, *Chem. Rev.* **1998**, *98*, 705.

[9] For example: [9a] J. A. Halfen, B. A. Jazdzewski, S. Mahapatra, L. M. Berreau, E. C. Wilkinson, L. Que, Jr., W. B. Tolman, *J. Am. Chem. Soc.* **1997**, *119*, 8217. [9b] Y. Wang, T. D. P. Stack, *J. Am. Chem. Soc.* **1996**, *118*, 13097. [9c] D. Zurita, I. Gautier-Luneau, S. Menage, J. L. Pierre, E. Saint-Aman, *J. Biol. Inorg. Chem.* **1997**, *2*, 46. [9d] E. Bill, J. Müller, T. Weyhermüller, K. Wieghardt, *Inorg. Chem.* **1999**, *38*, 5795 and references therein. [9e] M. A. Halcrow, L. M. Lindy Chia, X. Liu, E. J. L. McInnes, L. J. Yellowlees, F. E. Mabbs, I. J. Scowen, M. McPartlin, J. E. Davies, *J. Chem. Soc., Dalton Trans.* **1999**, 1753. [9f] S. Itoh, S. Takayama, R. Arakawa, A. Furuta, M. Komatsu, A. Ishida, S. Takamuku, S. Fukuzumi, *Inorg. Chem.* **1997**, *36*, 1407. [9g] K. Yamato, T. Inada, M. Doe, A. Ichimura, T. Takui, Y. Kojima, T. Kikunaga, S. Nakamura, N. Yanagihara, T. Onaka, S. Yano, *Bull. Chem. Soc. Jpn.* **2000**, *73*, 903. [9h] Y. Shimazaki, S. Huth, A. Odani, O. Yamauchi, *Angew. Chem. Int. Ed.* **2000**, *112*, 1666. [9i] M. Vaidyanathan, M. Palaniandavar, *Proc. Indian Acad. Sci. (Chem. Sci)* **2000**, *112*, 223. [9j] C. N. Verani, E. Bothe, D. Burdinski, T. Weyhermüller, U. Flörke, P. Chaudhuri, *Eur. J. Inorg. Chem.* **2001**, 2161.

[10] P. Chaudhuri, K. Wieghardt, *Progr. Inorg. Chem.* (Ed.: K. D. Karlin) **2002**, *50*, 151.

[11] B. F. Hoskins, R. Robson, D. Vince, *J. Chem. Soc., Chem. Commun.* **1973**, 392.

[12] R. K. Andrews, R. L. Blakeley, B. Zerner, in *The Bioinorganic Chemistry of Nickel* (Ed.: J. R. Lancaster), VCH, New York 1988.

[13] [13a] E. Jabri, M. B. Carr, R. P. Hausinger, P. A. Karplus, *Science* **1995**, *268*, 998. [13b] M. A. Pearson, L. O. Michel, R. P. Hausinger, P. A. Karplus, *Biochemistry* **1997**, *36*, 8164. [13c] S. Benini, W. R. Rypniewski, K. S. Wilson, S. Ciurli, S. Mangani, *J. Biol. Inorg. Chem.* **1998**, *3*, 268. [13d] S. Benini, W. R. Rypniewski, K. S. Wilson, S. Miletti, S. Ciurli, S. Mangani, *Structure* **1999**, *7*, 205. [13e] S. Ciurli, S. Benini, W. R. Rypniewski, K. S. Wilson, S. Miletti, S. Mangani, *Coord. Chem. Rev.* **1999**, *190−192*, 331.

[14] [14a] H. E. Wages, K. L. Taft, S. J. Lippard, *Inorg. Chem.* **1993**, *32*, 4985. [14b] Y. Hosokawa, H. Yamane, Y. Nakao, K. Matsumoto, S. Takamizawa, W. Mori, S. Suzuki, *Chem. Lett.* **1997**, 891. [14c] M. Arnold, D. A. Brown, O. Deeg, W. Errington, W. Haase, K. Herlihy, T. J. Kemp, H. Nimir, R. Werner, *Inorg. Chem.* **1998**, *37*, 2920. [14d] T. Koga, H. Furutachi, T. Nakamura, N. Fukita, M. Ohba, K. Takahashi, H. Okawa, *Inorg. Chem.* **1998**, *37*, 989. [14e] F. Meyer, H. Pritzkow, *Chem. Commun.* **1998**, 1555. [14f] F. Meyer, E. Kaifer, P. Kircher, K. Heinze, H. Pritzkow, *Chem. Eur. J.* **1999**, *5*, 1617. [14g] K. Yamaguchi, S. Koshino, F. Akagi, M. Suzuki, A. Uehara, S. Suzuki, *J. Am. Chem. Soc.* **1997**, *119*, 5752. [14h] H. Yamane, Y. Nakao, S. Kawabe, Y. Xie, N. Kanehisa, Y. Kai, M. Kinoshita, W. Mori, Y. Hayashi, *Bull. Chem. Soc. Jpn.* **2001**, *74*, 2107.

[15] A. M. Barrios, S. J. Lippard, *J. Am. Chem. Soc.* **2000**, *122*, 9172.

[16] [16a] K. E. Andrew, A. B. Blake, *J. Chem. Soc. A* **1969**, 1456. [16b] B. Aurivillius, *Acta Chem. Scand., Ser. A* **1977**, *31*, 501. [16c] J. A. Bertrand, C. Marabella, D. G. Vanderveer, *Inorg. Chim. Acta* **1978**, *26*, 113. [16d] W. L. Gladfelter, M. W. Lynch, W. P. Schaefer, D. N. Hendrickson, H. B. Gray, *Inorg. Chem.* **1981**, *20*, 2390. [16e] K. Bizilj, S. G. Hardin, B. F. Hoskins, P. J. Oliver, E. R. T. Tiekink, G. Winter, *Aust. J. Chem.* **1986**, *39*, 1035. [16f] L. Ballester, E. Coronado, A. Gutiérrez, A. Monge, M. F. Perpinán, E. Pinilla, T. Rico, *Inorg. Chem.* **1992**, *31*, 2053. [16g] A. J. Atkins, A. J. Blake, M. Schröder, *J. Chem. Soc., Chem. Commun.* **1993**, 1662. [16h] A. J. Blake, E. K. Brechin, A. Codron, R. O. Gould, C. M. Grant, S. Parsons, J. M. Rawson, R. E. P. Winpenny, *J. Chem. Soc., Chem. Commun.* **1995**,

1983. [16i] M. A. Halcrow, J.-S. Sun, J. C. Huffman, G. Christou, *Inorg. Chem.* **1995**, *34*, 4167. [16j] M. S. E. Fallah, E. Rentschler, A. Caneschi, D. Gatteschi, *Inorg. Chim. Acta* **1996**, *247*, 231. [16k] A. Escuer, M. Font-Bardiá, S. B. Kumar, X. Solans, R. Vicente, *Polyhedron* **1999**, *18*, 909. [16l] M. L. Tong, H. K. Lee, S.-L. Zheng, X.-M. Chen, *Chem. Lett.* **1999**, 1087. [16m] J. M. Clemente-Juan, B. Chansou, B. Donnadieu, J.-P. Tuchagues, *Inorg. Chem.* **2000**, *39*, 5515.

[17] For selected examples see: [17a] K. D. Karlin, A. Farooq, J. C. Hayes, B. I. Cohen, T. M. Rowe, E. Sinn, J. Zubieta, *Inorg. Chem.* **1987**, *26*, 1271. [17b] M. Sakamoto, S. Itose, T. Ishimori, N. Matsumoto, H. Okawa, S. Kida, *J. Chem. Soc., Dalton Trans.* **1989**, 2083. [17c] K. J. Oberhausen, J. F. Richardson, R. M. Buchanan, J. K. McCusker, D. N. Hendrickson, J.-M. Latour, *Inorg. Chem.* **1991**, *30*, 1357. [17d] S. S. Tandon, L. K. Thompson, J. N. Bridson, M. Bubenik, *Inorg. Chem.* **1993**, *32*, 4621. [17e] P. Cheng, D. Liao, S. Yan, J. Cui, Z. Jiang, G. Wang, *Helv. Chim. Acta* **1997**, *80*, 213. [17f] P. Amudha, M. Kandaswamy, L. Govindasamy, D. Velmurugan, *Inorg. Chem.* **1998**, *37*, 4486. [17g] P. Dalgaard, A. Hazell, C. J. McKenzie, B. Moubaraki, K. S. Murray, *Polyhedron* **2000**, *19*, 1909.

[18] [18a] J. A. Bertrand, J. A. Kelly, *J. Am. Chem. Soc.* **1966**, *88*, 4746. [18b] J. A. Bertrand, *Inorg. Chem.* **1967**, *6*, 495.

[19] [19a] H. Bock, H. tom Dieck, H. Pyttlik, M. Schnöller, *Z. Anorg. Allg. Chem.* **1968**, *357*, 54. [19b] B. T. Kilbourn, J. D. Dunitz, *Inorg. Chim. Acta* **1967**, *1*, 209. [19c] F. S. Keij, J. G. Haasnoot, A. J. Oosterling, J. Reedijk, C. J. O'Connor, J. H. Zang, A. L. Spek, *Inorg. Chim. Acta* **1991**, *181*, 185. [19d] H. M. Haendler, *Acta Crystallogr., Sect. C* **1990**, *46*, 2054. [19e] R. E. Norman, N. J. Rose, R. E. Stenkamp, *Acta Crystallogr., Sect. C* **1989**, *45*, 1707. [19f] S. Brownstein, N. F. Han, E. Gabe, F. Leer, *Can. J. Chem.* **1989**, *67*, 551. [19g] J. T. Guy, Jr., J. C. Cooper, R. D. Gillardi, J. L. Flippen-Anderson, C. F. George, Jr., *Inorg. Chem.* **1988**, *27*, 635. [19h] M. R. Churchill, F. J. Rotella, *Inorg. Chem.* **1979**, *18*, 853. [19i] R. C. Dickinson, F. T. Helm, W. A. Baker, Jr., T. D. Black, W. H. Watson, Jr., *Inorg. Chem.* **1977**, *16*, 1530 and references therein. [19j] J. J. de Boer, D. Bright, J. N. Helle, *Acta Crystallogr., Sect. B* **1972**, *28*, 3436. [19k] S. Teipel, K. Griesar, W. Haase, B. Krebs, *Inorg. Chem.* **1994**, *33*, 456. [19l] L. Chen, S. R. Breeze, R. J. Rousseau, S. Wang, L. K. Thompson, *Inorg. Chem.* **1995**, *34*, 454. [19m] S. R. Breeze, S. Wang, L. Chen, *J. Chem. Soc., Dalton Trans.* **1996**, 1341. [19n] A. M. Atria, A. Vega, M. Contreras, J. Valenzuela, E. Spodine, *Inorg. Chem.* **1999**, *38*, 5681.

[20] J. Reim, K. Griesar, W. Haase, B. Krebs, *J. Chem. Soc., Dalton Trans.* **1995**, 2649.

[21] F. Birkelbach, C. Krebs, V. Staemmler, unpublished, Bochum, Germany, **1997**.

[22] S. A. Marshall, A. R. Reinberg, *J. Appl. Phys.* **1960**, *31*, 3365.

[23] [23a] V. H. Crawford, H. W. Richardson, J. R. Wasson, D. H. Hodgson, W. E. Hatfield, *Inorg. Chem.* **1976**, *15*, 2107. [23b] L. Merz, W. Haase, *J. Chem. Soc., Dalton Trans.* **1980**, 875. [23c] L. K. Thompson, S. K. Mandal, S. S. Tandon, J. N. Bridson, M. K. Park, *Inorg. Chem.* **1996**, *35*, 3117 and references cited therein.

[24] P. Chaudhuri, C. N. Verani, E. Bill, E. Bothe, T. Weyhermüller, K. Wieghardt, *J. Am. Chem. Soc.* **2001**, *123*, 2213.

Received August 16, 2002
[I02463]